Numerical Simulation of Marangoni Convection around Gas Bubbles in a Liquid Matrix

Johannes Straub, Johann Betz, and Rudi Marek
Lehrstuhl A für Thermodynamik, Technische Universität München
Arcisstr. 21, D-8000 München 2, Germany

Abstract

Transient Marangoni convection under micro- and earth gravity conditions around a gas bubble floating in a liquid-filled rectangular box with adiabatic side walls, while the bottom and top walls are maintained at different temperatures, is simulated with a 2-dimensional model. Employing two numerical methods, a finite difference scheme with explicit time steps and a fully implicit control volume finite element method, the enhancement of the heat transfer in the liquid matrix due to Marangoni convection is investigated in parallel. To simplify the calculations, the bubble is fixed at a certain location in the container, while the necessary transient force to hold the bubble in place is determined. For a test fluid with $Pr = 1.93$, the transient overall heat transfer and fluid flow are examined for several configurations of bubble and container in terms of the dimensionless numbers Nu and Ma. Contrary to the very common view that the gas bubble would reduce the heat transfer due to its insulating behaviour, the energy transport is rather augmented by the Marangoni convection acting on the free surface of the bubble. Our numerical simulations show that Marangoni convection can fully replace buoyancy-induced heat transfer mechanisms in a microgravity environment. In contrast to former assumptions, Marangoni flow is, in general, not negligible. The transient development of fluid flow and heat transfer has fully been calculated, however, due to lack of space, only the final steady-state results are presented here.

Keywords: Transient numerical simulation - Marangoni convection - Surface phenomena - Heat transfer and fluid flow

1 Introduction

On a liquid surface, *Van der Waals* forces are responsible for surface tension, which strongly depends on the temperature of the liquid. For most liquids, the temperature gradient of surface tension is negative, and a flow, termed Marangoni or thermocapillary convection may be induced on plain or curved liquid-liquid or liquid-gas interfaces. Already in 1878, Marangoni [9] noted, "if, for some reason, a variation of surface tension occurs along a free surface, the fluid begins to move in the direction of increasing surface tension". For many years this effect has not been paid much attention to. Earlier investigations, especially in materials processing [6], [7], [11] and subcooled boiling under microgravity conditions [16], [18], [21] clearly demonstrated that Marangoni convection can fully replace buoyancy dominated heat transfer mechanisms. Numerical simulations of *Marek & Straub* [10] revealed that, even under earth gravity conditions, Marangoni flow cannot be overcome by natural convection in certain configurations. Depending on the boundary conditions, thermocapillary flow can either augment or counteract natural convection.

In many technical systems, it is highly desirable that convection substantially contributes to heat and mass transfer. Particularly, Marangoni convection can affect floating bubbles or droplets in a liquid matrix exposed to a temperature gradient. In 1959 Young et al. [20] investigated the motion of bubbles by adjusting a vertical temperature gradient in a fluid in such a way that the buoyancy of the bubble was compensated by the Marangoni force. However, the heat transfer was not considered. At first sight, one would expect a gas bubble floating in a liquid to significantly reduce the overall heat transfer due to its insulating behaviour. Taking thermocapillary flow into consideration, the question arises, if heat transfer through a liquid can be augmented by inserting a gas bubble.

The aim of our study is to investigate the heat transfer by thermocapillary convection around a gas bubble, frozen at a definite location in a rectangular enclosure with a vertical temperature gradient. Variable gravity conditions make it possible to study the interaction of buoyancy and surface tension-driven convection. The system under consideration is governed by the conservation laws for mass, momentum, and energy. As no analytical solution is possible, the governing equations are integrated numerically using a control volume finite difference method with explicit time steps, and for comparison purposes, a transient, fully implicit CV-FE method. In a first approximation, we reduce the three-dimensional problem to two dimensions by considering only a cross-section of the bubble. The special combination of a circular and a rectangular geometry excludes the use of a regular computational grid.

2 Nomenclature

B	width of the cavity
$Bo = Ra/Ma$	Bond number
c_p	isobaric specific heat capacity
F	force
$Fo = \frac{\alpha \cdot t}{L^2}$	Fourier number
g	gravitational acceleration (in y-direction)
h, H	height of the cavity
L	characteristic length (L=H for cases 1,2,3 — L=h for cases 4,5)
$Ma = -\frac{d\sigma}{dT} \cdot \frac{L \cdot \Delta T}{\alpha \cdot \eta}$	Marangoni number for the box
$Nu = \frac{L \cdot [T(y+\Delta y) - T(y)]}{\Delta T \cdot \Delta y}$	local Nusselt number
p	pressure
$Pr = \frac{\nu}{\alpha} = \frac{\eta \cdot c_p}{\lambda}$	Prandtl number
R	bubble radius

Proceedings VIIIth European Symposium on Materials and Fluid Sciences in Microgravity, Brussels, Belgium, 12 - 16 April 1992, ESA SP-333 (August 1992)

$Ra = \frac{g \cdot \beta_p \cdot \Delta T \cdot L^3}{\nu \cdot \alpha}$	Rayleigh number for the box
t	time
T	temperature
u	x-velocity
u_r	radial velocity on the bubble surface
u_φ	azimuthal velocity on the bubble surface
v	y-velocity
α	thermal diffusivity
β_p	thermal expansion coefficient
η	dynamic viscosity
λ	thermal conductivity
ν	kinematic viscosity
ϱ	density of the liquid
τ	shear stress
σ	surface tension
$\frac{d\sigma}{dT}$	temperature coefficient of surface tension
$\Delta T = T_t - T_b$	temperature difference in the box

subscripts:

b	bottom wall
cold	cold wall
g	gas
hot	hot wall
l	liquid
M	Marangoni
r	radial
t	top wall
0	reference value
φ	azimuthal

3 Physical Model

As a first approximation of the problem of thermocapillary flow around an enclosed gas bubble, the configuration of a rectangular container with an ideally spherical air bubble floating in a liquid, as sketched in Fig. 1, is studied. Assuming rotationally symmetrical flow around the bubble, the three-dimensional fluid flow and heat transfer is regarded only in a cross-section through the centre of the bubble (Fig. 1). This truncation to two dimensions yields an enormous gain in computing time and memory, while all important three-dimensional effects can be shown.

Due to the relative small values for the transport properties η and λ and the density ϱ of the gas, heat transfer and fluid flow are neglected in the bubble, and are only considered in the liquid as an interaction of Marangoni and natural convection.

Conservation Laws

Using the *Boussinesq* approximation [5], originally proposed by *Overbeck* [12], for the properties of the surrounding liquid, the following coupled conservation laws apply [4]:

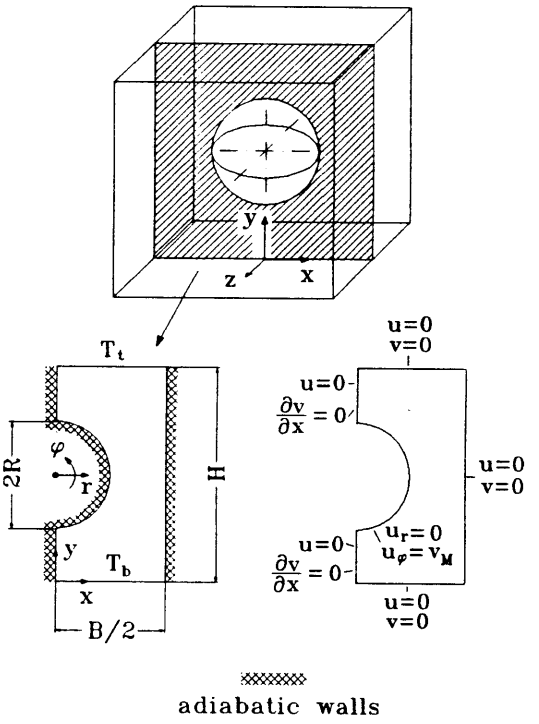

Figure 1: Computational domain of the three-dimensional heat transfer problem with corresponding boundary conditions

mass

$$\frac{1}{\varrho}\frac{\partial \varrho}{\partial t} + \frac{\partial u}{\partial x} + \frac{\partial v}{\partial y} = 0 \qquad (1)$$

energy

$$\frac{\partial T}{\partial t} + u\frac{\partial T}{\partial x} + v\frac{\partial T}{\partial y} = \alpha\left(\frac{\partial^2 T}{\partial x^2} + \frac{\partial^2 T}{\partial y^2}\right) \qquad (2)$$

x-momentum

$$\frac{\partial u}{\partial t} + u\frac{\partial u}{\partial x} + v\frac{\partial u}{\partial y} = -\frac{1}{\varrho}\frac{\partial p}{\partial x} + \nu\left(\frac{\partial^2 u}{\partial x^2} + \frac{\partial^2 u}{\partial y^2}\right) \qquad (3)$$

y-momentum

$$\frac{\partial v}{\partial t} + u\frac{\partial v}{\partial x} + v\frac{\partial v}{\partial y} = g - \frac{1}{\varrho}\frac{\partial p}{\partial y} + \nu\left(\frac{\partial^2 v}{\partial x^2} + \frac{\partial^2 v}{\partial y^2}\right) \qquad (4)$$

Boundary and Initial Conditions

The governing boundary conditions for the cross-section in Fig. 1 are:

Thermal boundary conditions: As the thermal conductivity of air is small compared to that of the surrounding liquid, the surface of the bubble is assumed to be adiabatic. Moreover, heat transfer by radiation is neglected, since the maximum temperature differences of 3.4 K in the system are small; heat is only transported by conduction and convection in the liquid. The bottom and

top walls of the enclosure are kept at constant, but different temperatures, while the side walls are assumed to be perfectly insulated:

$$T(y=0) = T_b \quad \wedge \quad T(y=H) = T_t$$
$$\frac{\partial T}{\partial x} = 0 \Big|_{x=0, x=B/2} \quad \wedge \quad \frac{\partial T}{\partial r} = 0 \Big|_{r=R} \quad \wedge \quad \frac{\partial T}{\partial z} = 0 \qquad (5)$$

Hydrodynamic boundary conditions: We assume non-slip conditions at all rigid walls. Furthermore, no mass is transported over the interface of the bubble:

$$u = v = 0 \Big|_{x=B/2, y=0, y=H} \quad \wedge \quad u = 0 \Big|_{x=0} \quad \wedge \quad u_r = 0 \Big|_{r=R}$$
$$\frac{\partial v}{\partial x} = 0 \Big|_{x=0} \quad \wedge \quad \frac{\partial u}{\partial z} = 0 \quad \wedge \quad \frac{\partial v}{\partial z} = 0 \qquad (6)$$

Applying *Newton's* law of viscosity and considering the fact that $\tau_g \ll \tau$, a balance between viscous shear stresses and surface tension forces on the free surface in azimuthal direction yields the so-called Marangoni boundary condition [16]:

$$\tau + \tau_g \approx \tau \approx \frac{1}{R}\frac{\partial \sigma}{\partial \varphi} \approx \frac{1}{R}\frac{\partial T}{\partial \varphi}\frac{d\sigma}{dT} \approx \eta \left[\frac{\partial u_\varphi}{\partial r} - \frac{u_\varphi}{r}\right]\Big|_{r=R} \qquad (7)$$

Initially, the liquid in the container is at rest and the temperature distribution is described by a linear profile in y-direction with isothermal cross-sections for $y = \text{const.}$, equivalent to steady-state heat conduction in a box with isothermal top and bottom, and adiabatic side walls.

Other Thermophysical Properties

We used water at a mean temperature of 365 K as a test fluid in our calculations, even if, for some other reasons, Marangoni convection is not always observed in water [16]. The small temperature differences up to 1.7 K from the mean temperature of the liquid in a range of $0 < Ma \leq 250000$, and the great distance to the critical point justify the use of a constant temperature gradient of surface tension. A series of calculations was performed to examine the influence of a constant and a variable temperature coefficient of surface tension. The deviations in the steady-state overall Nusselt number between calculations with $\frac{d\sigma}{dT} = \frac{d\sigma}{dT}(T)$ and $\frac{d\sigma}{dT} = \text{const.}$ are less than 0.01 %. The thermophysical properties of the test liquid are shown in Tab. 1.

c_p	4206.9	$\frac{J}{kgK}$
λ	0.673	$\frac{W}{mK}$
η	$308.64 \cdot 10^{-6}$	$\frac{Ns}{m^2}$
ϱ	963.84	$\frac{kg}{m^3}$
β_p	$7.116 \cdot 10^{-4}$	$\frac{1}{K}$
$\frac{d\sigma}{dT}$	$-1.8892 \cdot 10^{-4}$	$\frac{N}{mK}$

Table 1: Thermophysical properties of the test liquid ($Pr = 1.93$)

4 Mathematical Model

Implicit and semi-implicit numerical methods are frequently preferred to explicit schemes in transient fluid flow calculations, since time steps of arbitrary size can be chosen. However, their computational effort is greater, and sometimes an iterative solution is necessary. Explicit methods, on the other hand, can easily be implemented, and their computational simplicity can make up for the limitation of the time step by stability criteria. Here, two numerical methods were implemented in parallel. On the one hand, a finite volume scheme with explicit time steps, power-law differences, and the SIMPLE algorithm for the pressure-velocity coupling was employed. On the other hand, an extended fully implicit TCV-FE method (Transient Control-Volume Finite-Element Method), based on the ideas of *Baliga et al.* [3] and *Prakash et al.* [14], with exponential differences and the SIMPLE algorithm was developed for the 2-dimensional laminar heat transfer and fluid flow problem.

Computational Grid

Resorting to a well-tested explicit finite difference computer code for transient heat transfer and fluid flow problems in rectangular domains, the circular geometry of the bubble and the rectangular cavity in Fig. 1 were discretized using "blocked-off regions" [13] in connection with regular triangular elements. Temperature and pressure are calculated in the centre of a control volume of this grid, which is therefore denoted "energy grid" (Fig. 2). For velocities, a "staggered" or "displaced grid" according to *Harlow & Welch* [8], and *Patankar* [13] is utilized. To approximate the spherical shape of the bubble as accurately as possible, and to minimize the discretization errors in the calculation domain, the right half of the sectional areas in Figs. 1 and 3 is discretized with 50 grid points in horizontal and, for flat containers, with 50 nodes in vertical direction; for cubic enclosures 100 grid points were provided in vertical direction.

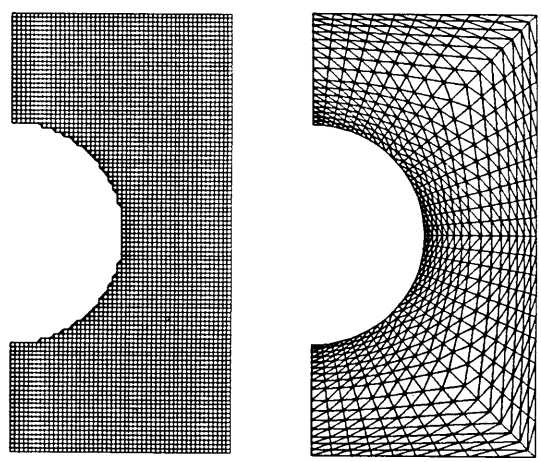

Figure 2: Numerical grid with 50 * 100 control volumes and approximation of the bubble surface with regular triangular elements (left), and grid for the TCV-FE method (right)

In the TCV-FEM formulation, the domain of interest is divided into three-node triangular elements, while the

curved bubble surface is piecewisely approximated by straight lines. All primitive variables T,u,v,p are stored at the nodes of the triangular elements. To avoid the problem of a checkerboard pressure field, a co-located variable arrangement, based on the work of *Prakash et al.* [14], was chosen. To resolve the steep velocity gradients at the bubble surface due to Marangoni convection very accurately, a local refinement of the grid (Fig. 2) turned out to be very profitable.

5 Results

Decaying Flow Behaviour

Varying *Ma* and *Ra* via the temperature gradient in the container, we performed case studies of Marangoni convection and the corresponding heat transfer around the bubble for some selected configurations (Fig. 3) both under micro- and earth gravity conditions.

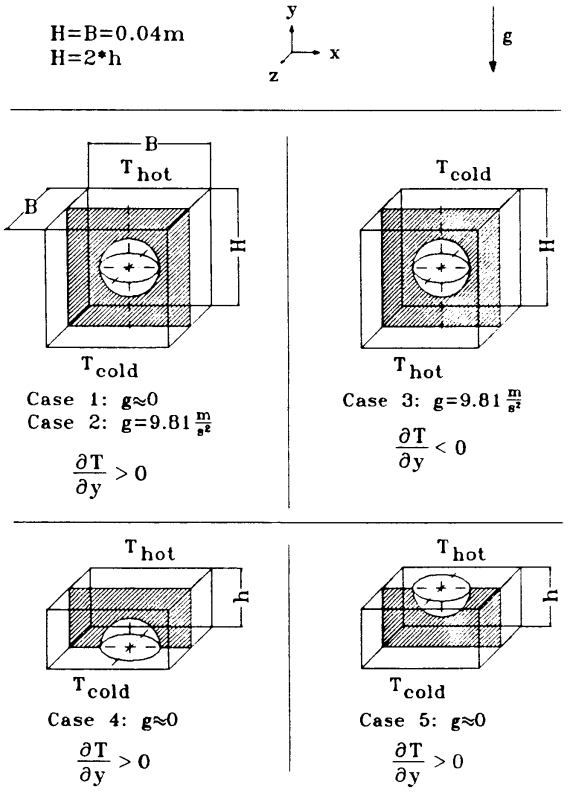

Figure 3: Overview of studied configurations

Case 1: Pure Marangoni convection (M) around a spherical bubble in the centre of a cubic container under microgravity ($g \approx 0$).

Case 2: Marangoni flow acting against buoyancy convection (M−B) around a spherical bubble frozen in the centre of a cubic container under earth gravity ($\frac{\partial T}{\partial y} > 0$).

Case 3: Marangoni convection acting in the direction of buoyancy flow (M+B) around a spherical bubble frozen in the centre of a cubic container under earth gravity ($\frac{\partial T}{\partial y} < 0$).

Case 4: Pure Marangoni convection (M) around a hemispherical bubble on the bottom wall of a flat container under microgravity ($g \approx 0$).

Case 5: Pure Marangoni convection (M) around a hemispherical bubble on the top wall of a flat container under microgravity ($g \approx 0$).

For all cases studied, the average computing time on a CRAY Y-MP 4/432 supercomputer amounted to about 1000 CPU-seconds for a given Marangoni number. Due to lack of space here, only steady-state results are presented for cases 2 through 5, although the transient development of the flow and temperature fields has fully been investigated.

Thermocapillary convection expands from the bubble's interface both into the interior of the bubble and into the surrounding liquid by viscous shear stresses. As stated above, the fluid flow and heat transfer inside the gas bubble are negligible for most air-liquid-combinations. The rigid container walls give rise to a recirculating flow in the liquid, illustrated in Figs. 4, and 6-9 together with the corresponding isotherms. All velocity vectors are related to the occurring maximum velocity in the system, thus comparisons between different flow patterns cannot necessarily be drawn.

The temperature field around the bubble is strongly coupled with the flow field. When the Marangoni number or the temperature difference between bottom and top walls of the container, respectively, is increased, the influence of thermocapillary convection on heat transfer grows, and the isotherms accumulate near the heated and cooled walls. The number of isotherms originating from the bubble decreases with increasing Marangoni number (Figs. 4, and 6-9), which is in accordance with [16]. The computations thus clearly account for the effect that Marangoni convection around gas bubbles reduces its own driving temperature gradients.

The behaviour of Marangoni convection under earth gravity conditions is very noticeable. In case 2, a stable vertical density stratification is initially present in the enclosure. The displacement of the isotherms in Fig. 8 demonstrates the effect Marangoni convection exerts on buoyancy flow. For $\frac{d\sigma}{dT} < 0$, fluid particles are driven against the direction of natural convection, and this flow pattern still prevails, when the number of isotherms originating from the free surface is reduced at higher Marangoni numbers. Recently, *Straub et al.* [16] presented some experimental results for this phenomenon. On the other hand, compared to micro-gravity conditions (Fig. 4), buoyancy displaces the bulk flow towards the bubble surface. In case 3, an unstable density stratification is chosen as initial condition in the box, so that Marangoni and buoyancy convection augment each other. Due to the reversed temperature gradient in the enclosure, surface tension-driven convection acts in the opposite direction compared to cases 1 and 2. Fig. 9 illustrates that, even for small Marangoni numbers, the recirculating flow pattern prevails over a large part of the liquid.

The accumulation of isotherms at the heated and cooled walls is equivalent to an increase in the local and global Nusselt numbers at those walls. In order to demonstrate the enhancement of the heat transfer in the box by thermocapillary convection, the steady-state Nusselt number *Nu* at the isothermal bottom and top walls is depicted as a function of the Marangoni number *Ma* for the cases 1 through 5 in Fig. 10.

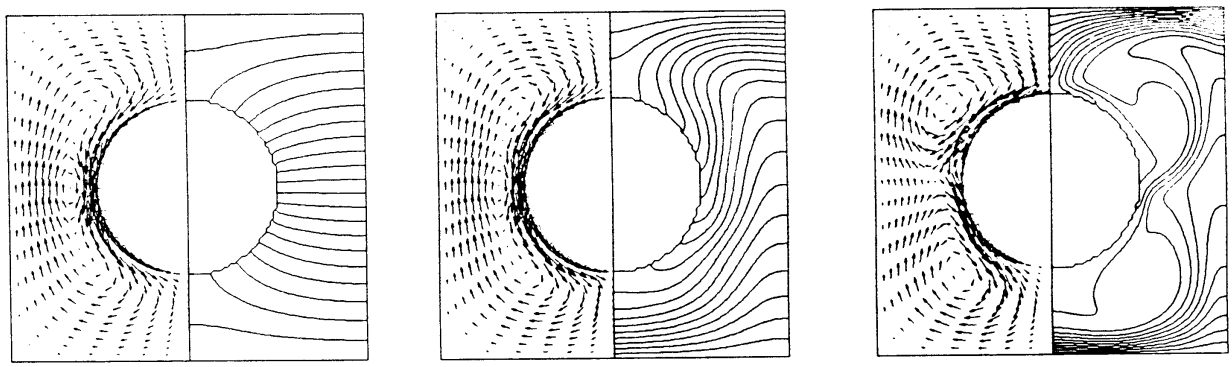

Figure 4: Predicted velocity fields and isotherms for case 1 (M): $Ma = 10$ (left), $Ma = 5000$ (middle), $Ma = 100000$ (right), $Ra \approx 0$

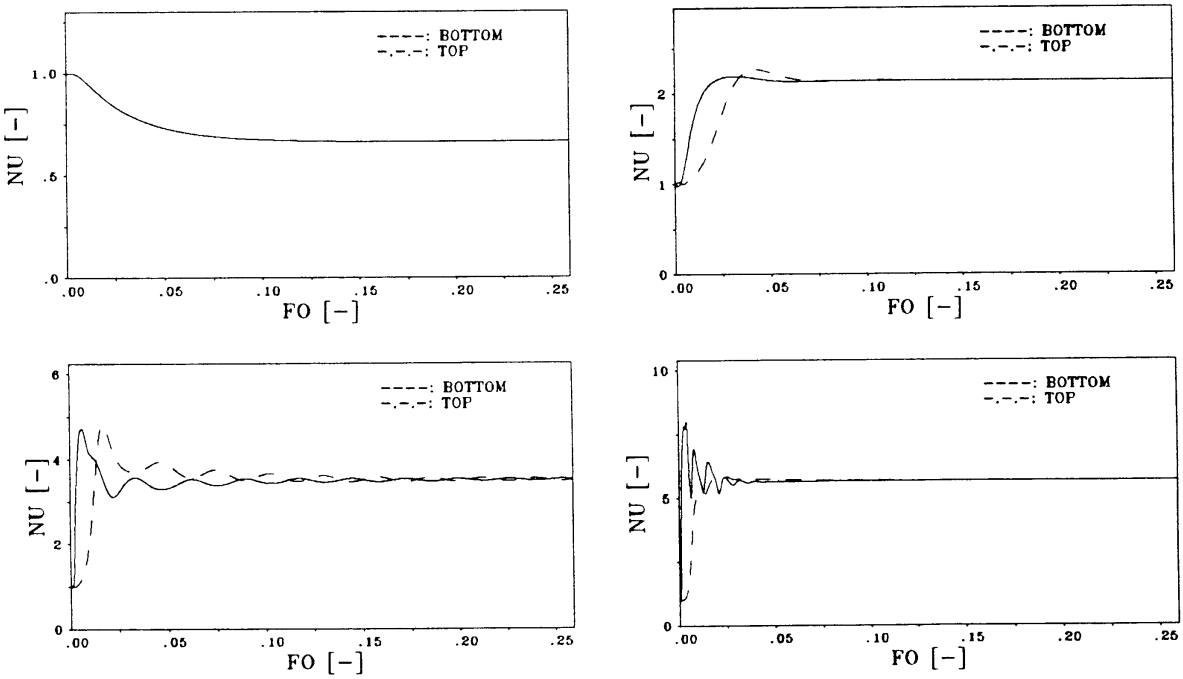

Figure 5: Transient development of the Nusselt number at the isothermal bottom and top walls for case 1, $g \approx 0$, $Ma = 10$ (left top), $Ma = 5000$ (right top), $Ma = 25000$ (left bottom), $Ma = 100000$ (right bottom).

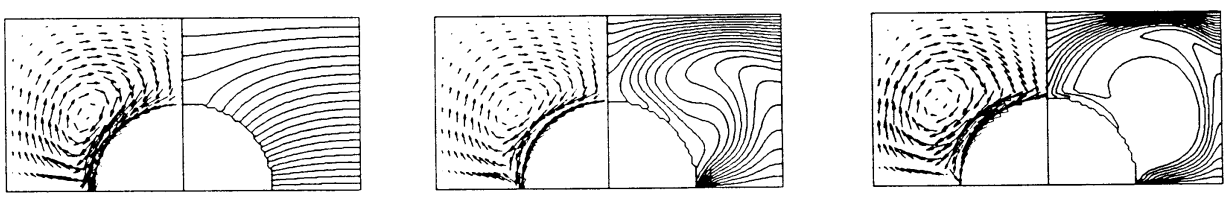

Figure 6: Predicted velocity fields and isotherms for case 4 (M): $Ma = 10$ (left), $Ma = 10000$ (middle), $Ma = 250000$ (right), $Ra \approx 0$

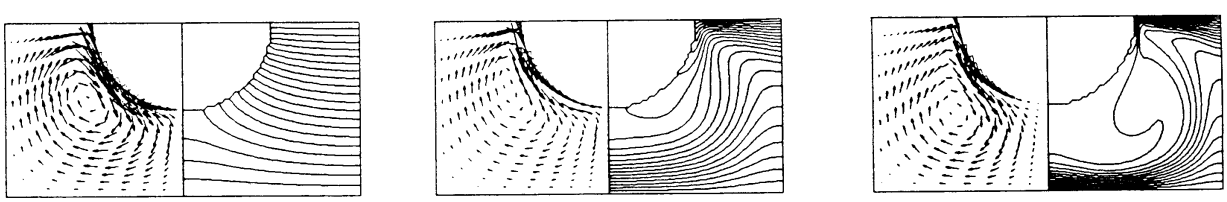

Figure 7: Predicted velocity fields and isotherms for case 5 (M): $Ma = 10$ (left), $Ma = 5000$ (middle), $Ma = 50000$ (right), $Ra \approx 0$

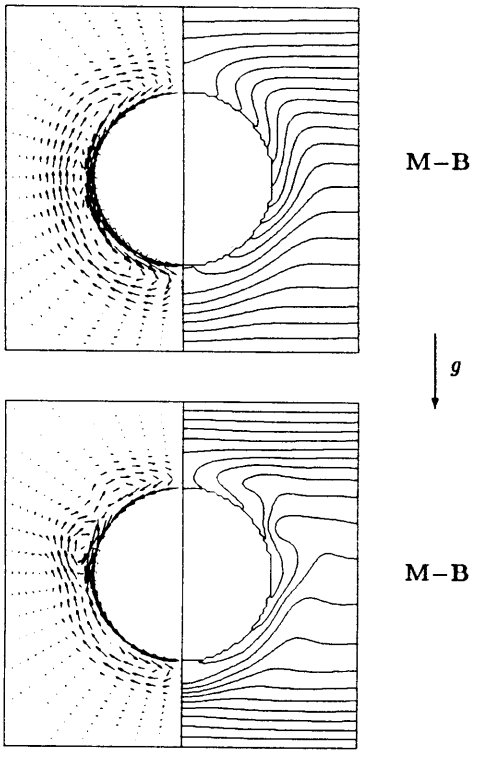

Figure 8: Predicted velocity fields and isotherms for case 2 (**M–B**): $Ma = 10000$, $Ra = 5.7 \cdot 10^5$ (top), $Ma = 100000$, $Ra = 5.7 \cdot 10^6$ (bottom).

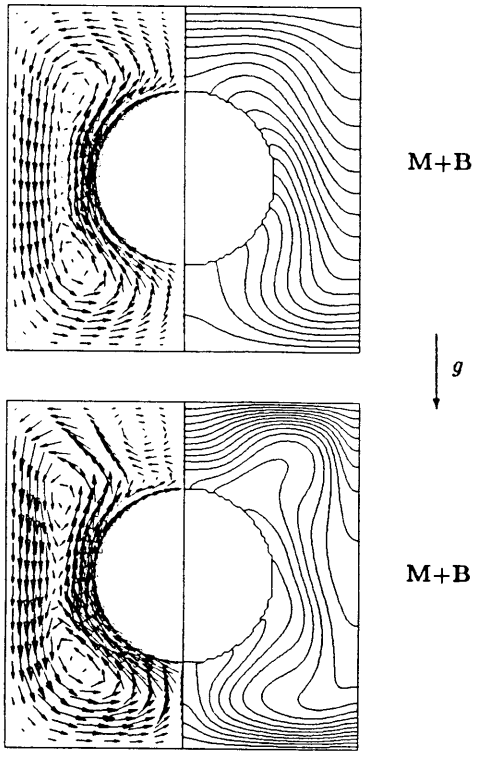

Figure 9: Predicted velocity fields and isotherms for case 3 (**M+B**): $Ma = 1000$, $Ra = 5.7 \cdot 10^4$ (top), $Ma = 5000$, $Ra = 2.8 \cdot 10^5$ (bottom).

To examine the influence of the gas bubble on the transient development of the heat transfer in the box, we utilized a temperature field constant in x- and z-directions

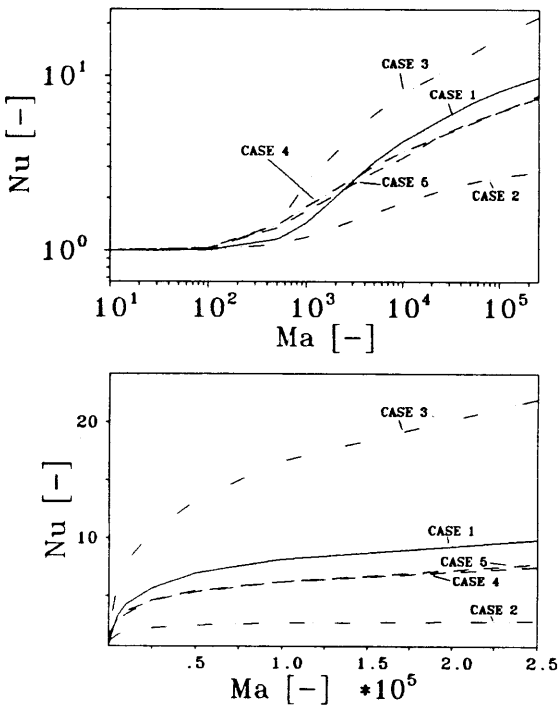

Figure 10: Overall steady-state Nusselt number Nu at the isothermal walls of the container as a function of the Marangoni number Ma for the cases investigated ($Pr = 1.93$).

with a constant gradient in y-direction for the whole calculation domain for $t = 0$, as it prevails in the steady-state case of pure heat conduction in the liquid-filled container without bubble. For small Marangoni numbers, the absolute velocities in the liquid are very moderate, hence diffusive heat transfer is dominant over convective energy transport. The insulating effect of the air bubble reduces the heat transfer in the enclosure to 67.5% ($Nu_0 = 0.675$) of the value for pure steady-state heat conduction in a box of the same size *without* bubble only filled with liquid ($Nu = 1.0$). This behaviour is depicted in Fig. 5. For an easier understanding, we scaled all Nusselt numbers with the reference value of $Nu_0 = 0.675$ for steady-state heat conduction in a box *with* bubble shown in Fig. 1. Thus, $Nu = 1$ refers to $Nu_0 = 0.675$. The reduction of heat transfer by 32.5% in the case of pure heat conduction ($Ma \rightarrow 0$) was obtained by both the two-dimensional flow calculation described above (Fig. 4) and by employing the TCV-FE scheme. Furthermore, the calculated results agree with an investigation by *Riedle et al.* [15].

For a growing Marangoni number, convection dominates over heat conduction resulting in an increase of the Nusselt number at the heated and cooled walls for $t > 0$ (Fig. 5). As shown in Fig. 10, the steady-state Nusselt number Nu at the isothermal container walls increases with growing Marangoni number Ma, when a certain time is reached. However, for higher Marangoni numbers this increase of the Nusselt number is getting smaller. The reason for this behaviour is the reduction of the important temperature gradients near the free surface by Marangoni convection itself, which occurs to a much greater extent for high Marangoni numbers.

6 Force on the Bubble

As mentioned earlier, the movement of bubbles or drops in a fluid matrix under a temperature gradient is known from the experimental [19],[20] and theoretical [17] works of other authors. For most liquid-liquid and liquid-gas combinations, a bubble migration towards the warmer liquid is observed under microgravity. This transient bubble motion could have been simulated with our program as well, however, the generation of a new grid at each time step would have consumed large amounts of CPU time. Thus, the bubble is regarded as fixed at a certain location in the enclosure, and the force necessary to hold the bubble in place is determined. The following stress components act on the bubble surface:

- Hydrostatic and hydrodynamic pressure resulting from the fluid flow outside and inside the bubble
- Tangential shear stress on the liquid and gas sides of the bubble
- Normal shear stress resulting from velocity gradients and the viscosity of the liquid and the gas

A more detailed description of bubble forces has been worked out by *Szymczyk* [17] and is not be repeated here.

Assuming a rotationally symmetric fluid flow around the bubble and neglecting the gas forces inside the bubble because of its small density and viscosity, a bubble force F can be easily obtained by integrating along the interface with the trapezoidal rule and adding up all the force components. As shown in Fig. 11, the steady-state force on the fixed bubble of case 1 is a function of the Marangoni number Ma. For higher Marangoni numbers, the increase of the bubble force is getting smaller, because the temperature gradients necessary for the fluid flow near the free surface are reduced by Marangoni convection itself. On the earth, for the cases 2 and 3 (Fig. 3), and a range of $0 < Ma \leq 250000$, the buoyancy on the gas bubble is a dominant force component, while other components become negligible. On the other hand, *Young et al.* [20] pointed out that the situation may completely be different for smaller bubbles.

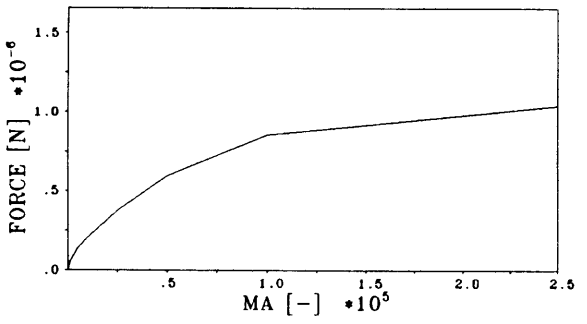

Figure 11: Force F acting on the fixed bubble of case 1 as a function of the Marangoni number Ma.

7 Conclusion

In the previous section, the enhancement of the heat transfer in a rectangular container by thermocapillary convection was established quantitatively in terms of the steady-state Nusselt number Nu and the Marangoni number Ma for some selected bubble-container configurations and a liquid with $Pr = 1.93$. Two numerical methods were employed to ensure the validity of the presented results. The obtained findings once more clearly emphasize the importance of thermocapillary convection for the heat transfer in liquids both under micro- and earth gravity.

Future investigations will focus on a universal description of the enhancement of heat transfer by Marangoni convection with dimensionless quantities *Marangoni*, *Fourier*, *Rayleigh*, *Nusselt*, *Prandtl*, and *Froude* obtained from the dimensionless conservation laws for energy and momentum.

Parameters not, or only partially considered yet, are the size of the bubble (ratio R/H), its location in the container, the physical properties of the liquid (Pr), the ratio of natural and Marangoni convection (Bond number $Bo = Ra/Ma$), and the geometry of the container (ratio H/B).

Acknowledgement

Essentially, this paper is an excerpt of the diploma thesis of the second author. The first and third authors are supported by the DFG (Deutsche ForschungsGemeinschaft) through grant Str 117/29-1, further theoretical and experimental investigations of heat transfer by thermocapillary convection and the development of the TCV-FEM scheme are supported by the DFG through grant Str 117/34-1 which is gratefully acknowledged.

References

[1] R. B. Baliga, A Control-Volume Based Finite Element Method for Convective Heat and Mass Transfer, Ph.D. thesis, University of Minnesota, Minneapolis, 1978.

[2] R. B. Baliga, and S. V. Patankar, A Control Volume Finite-Element Method for Two-Dimensional Fluid Flow and Heat Transfer, *Numerical Heat Transfer*, vol. 6, pp. 245-261, 1983.

[3] R. B. Baliga, and S. V. Patankar, Elliptic Systems: Finite-Element Method II, *Handbook of numerical Heat Transfer*, John Wiley & Sons, Inc., New York, pp. 421-461, 1988.

[4] B. R. Bird, W. E. Stewart, and E. N. Lightfoot, *Transport Phenomena*, John Wiley & Sons Inc., New York, London, 1960.

[5] J. V. Boussinesq, *Théorie analytique de la chaleur*, vol. 2, Gauthier-Villard, Paris, 1903.

[6] C.-H. Chun, Numerical Study on the Thermal Marangoni Convection and Comparison with Experimental Results from the TEXUS-Rocket Program, *Acta Astronautica*, vol. 11, nos. 3-4, pp. 227-232, 1984.

[7] P. Hammerschmid, Bedeutung des Marangoni-Effekts für metallurgische Vorgänge, *Stahl und Eisen*, vol. 107, no. 2, pp. 61-66, 1987.

[8] F. H. Harlow, and E. J. Welch, Numerical Calculation of Time-Dependent Viscous Incompressible Flow of Fluid with Free Surface, *The Physics of Fluids*, vol. 8, no. 12, pp. 2182-2189, 1965.

[9] C. G. M. Marangoni, Verteidigung der Theorie der Oberflächenelasticität der Flüssigkeiten. Oberflächenplasticität, *Beiblätter zu Poggendorff's Annalen der Physik und Chemie*, vol. 3, 1878, no. 12, pp. 842-846.

[10] R. Marek, and J. Straub, Three-Dimensional Transient Simulation of Marangoni Flow in a Cylindrical Enclosure under Various Gravity Levels, *Microgravity Science and Technology*, vol. 4, no. 2, pp. 153-154, Sept. 1991.

[11] J. Martinez, J. M. Haynes, and D. Langbein, Fluid Statics and Capillary in Fluid Science and Material Science in Space, H. U. Walter (ed.), *Fluid Sciences and Material Sciences in Space*, Berlin, Heidelberg, New York, Springer Verlag, 1987.

[12] A. Overbeck, Über die Wärmeleitung der Flüssigkeiten bei Berücksichtigung der Strömungen infolge von Temperaturdifferenzen, *Annalen der Physik und Chemie, Neue Folge*, vol. 7, pp. 271-292, 1879.

[13] S. V. Patankar, *Numerical Heat Transfer and Fluid Flow*, Hemisphere Publishing Corporation, Washington, London, 1980.

[14] C. Prakash, and S. V. Patankar, A Control Volume-Based Finite-Element Method for solving the Navier-Stokes Equations using Equal-Order Velocity-Pressure Interpolation, *Numerical Heat Transfer*, vol. 8, pp. 259-280, 1985.

[15] K. Riedle, H. Sebulke, and U. Grigull, Formkoeffizient des Wärmestroms in gelochten Flanschen und Streifen, *Thermo- and Fluid Dynamics*, vol. 3, pp. 70-74, 1970.

[16] J. Straub, A. Weinzierl, and M. Zell, Thermokapillare Grenzflächenkonvektion an Gasblasen in einem Temperaturgradienten, *Thermo- and Fluid Dynamics*, vol. 25, pp. 281-288, 1990.

[17] J. A. Szymczyk, *Berechnung der thermokapillaren Blasenbewegung in Flüssigkeiten unter Schwerelosigkeit für große Reynolds- und Marangonizahlen*, dissertation, Universität-Gesamthochschule Essen, 1985.

[18] A. Weinzierl, *Untersuchung des Wärmeübergangs und seiner Transportmechanismen bei Siedevorgängen unter Mikrogravitation*, dissertation, Lehrstuhl A für Thermodynamik, Technische Universität München, 1984.

[19] G. Wozniak, *Experimentelle Untersuchung des Einflusses der Thermokapillarität auf die Bewegung von Tropfen und Blasen*, dissertation, Universität-Gesamthochschule-Essen, 1986.

[20] N. O. Young, J. S. Goldstein and M. J. Block, The Motion of Bubbles in a Vertical Temperature Gradient, *Journal of Fluid Mechanics*, vol. 6, pp. 350-356, 1959.

[21] M. Zell, *Untersuchung des Siedevorgangs unter Mikrogravitation*, dissertation, Lehrstuhl A für Thermodynamik, Technische Universität München, 1991.